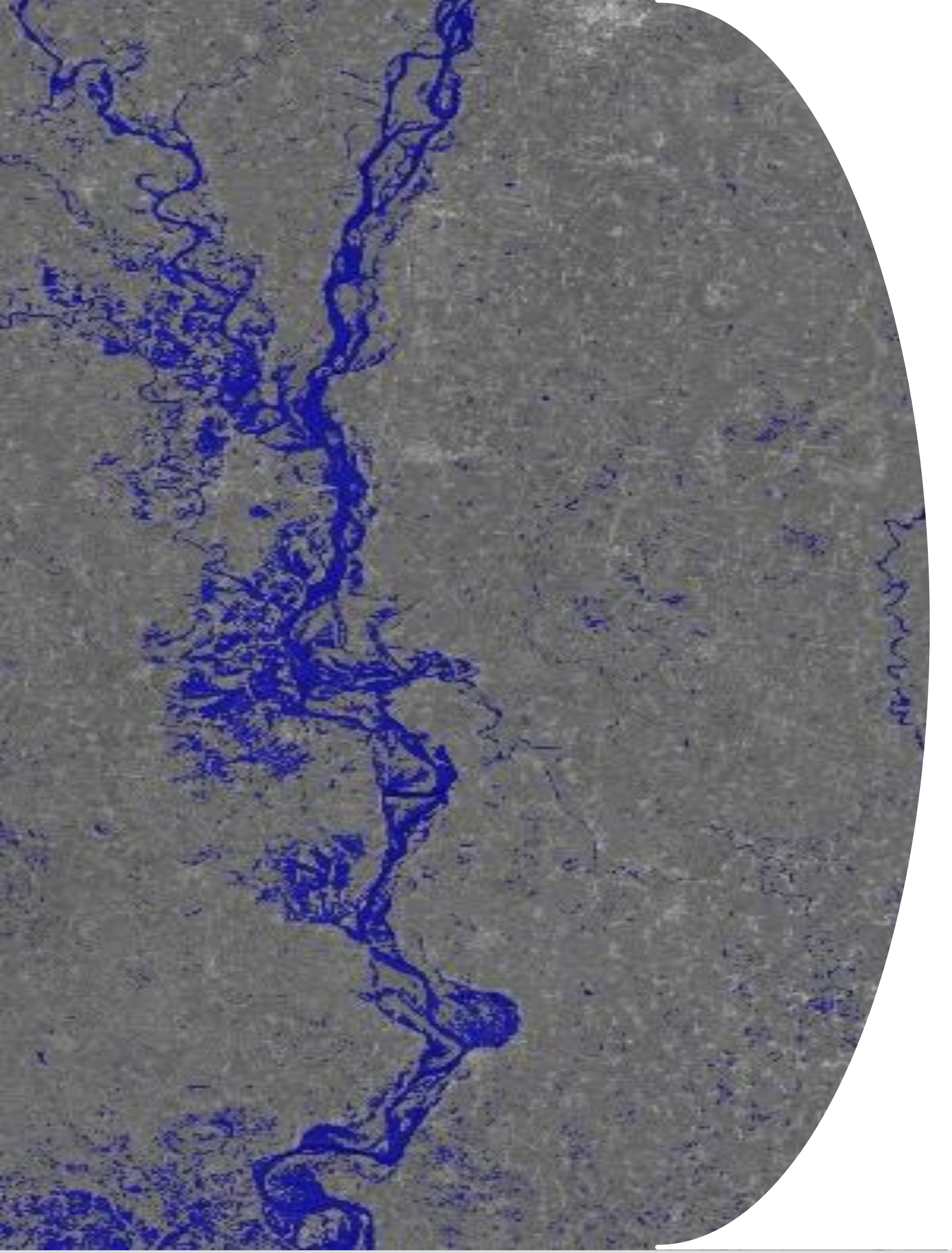

AI-Driven Flood Inventory Generation from Multi-Source Remote Sensing for Reliable Susceptibility Mapping

Armin Moghimi, Ph.D. Department of Geography, K. N. Toosi University of Technology; Ludwig-Franzius-Institut, Leibniz University Hannover

8th September 2025

Floods: A Major Global Hazard

Why Floods Matter

- 🌍 Most frequent climate-related disaster
- 📈 Increasing frequency & intensity due to climate change
- 💰 Huge economic lsses (billions annually)
- 👥 High human impact (displacement, fatalities, livelihoods)

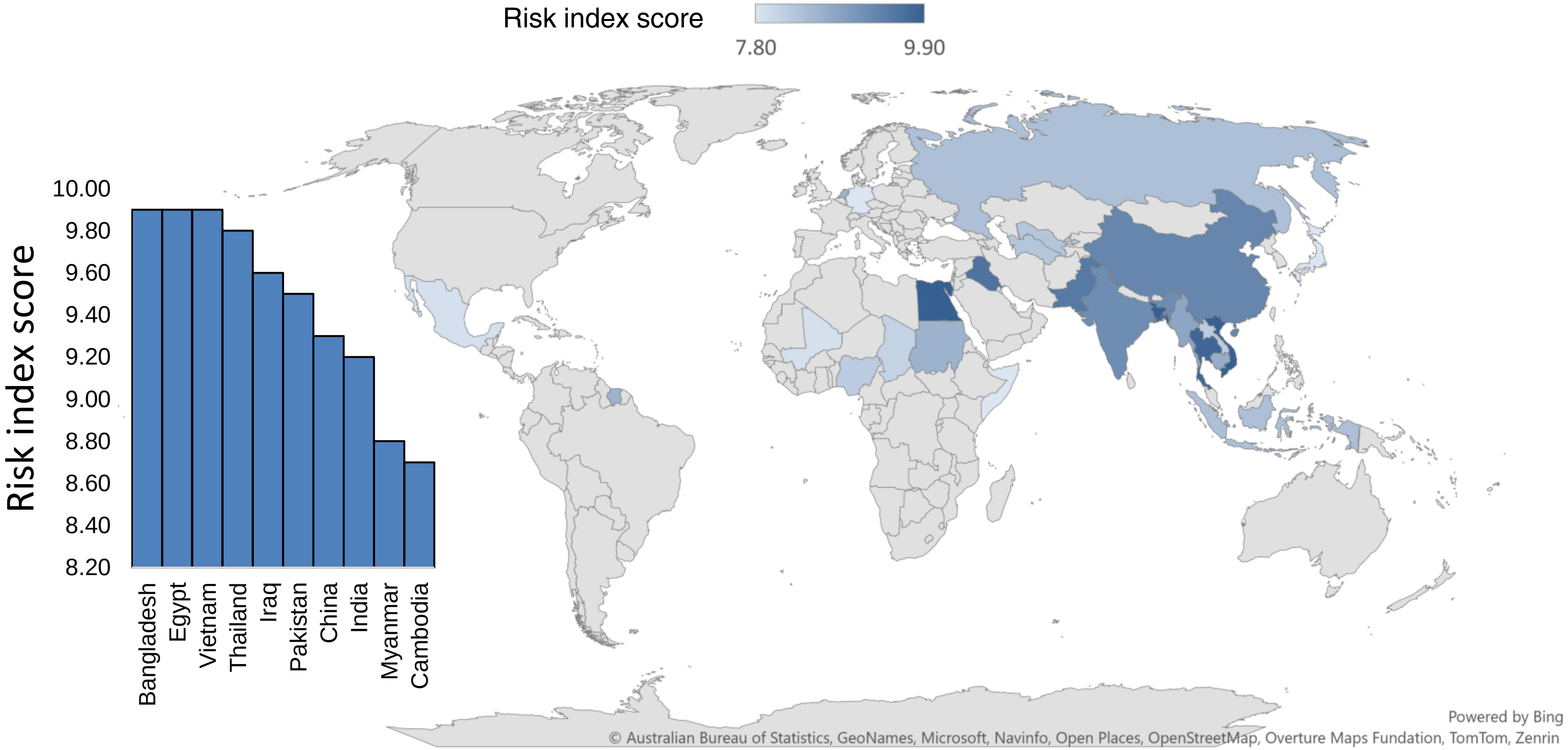

Source: European Commission. (March 31, 2025). In *Statista*. Retrieved September 06, 2025, from https://www.statista.com/statistics/1306264/countries-most-exposed-to-floods-by-risk-index-score/

Date	19 March 2019 – 29 April 2019
Location	Fars province Golestan province Mazandaran province Khuzestan province Lorestan province Ilam province and 20 other provinces.
Deaths	77+ deaths, 791 injured,
Property damage	•$4.1 billion (2019 USD) About 1,900 cities and villages damaged •78 roads had been blocked and 84 bridges in flood-stricken areas affected

Source: https://en.wikipedia.org/wiki/2019_Iran_floods
https://www.mehrnews.com/

Floods: Flood Susceptibility Mapping

What is Flood Susceptibility Mapping?
•Identifies **areas most likely to experience flooding**
•Based on **historical flood data + environmental factors** (rainfall, topography, soil, land use)
•Produces **probability maps** showing high, medium, and low susceptibility zones

Why It Matters:
•☑ Supports **urban planning** and land-use management
•☑ Informs **disaster preparedness & emergency response**
•☑ Aids in **infrastructure protection & insurance planning**
•☑ Reduces **loss of lives and property** through proactive action

Key Idea:
Flood susceptibility maps ≠ show when floods occur,
but they do show **where floods are more likely to occur**.

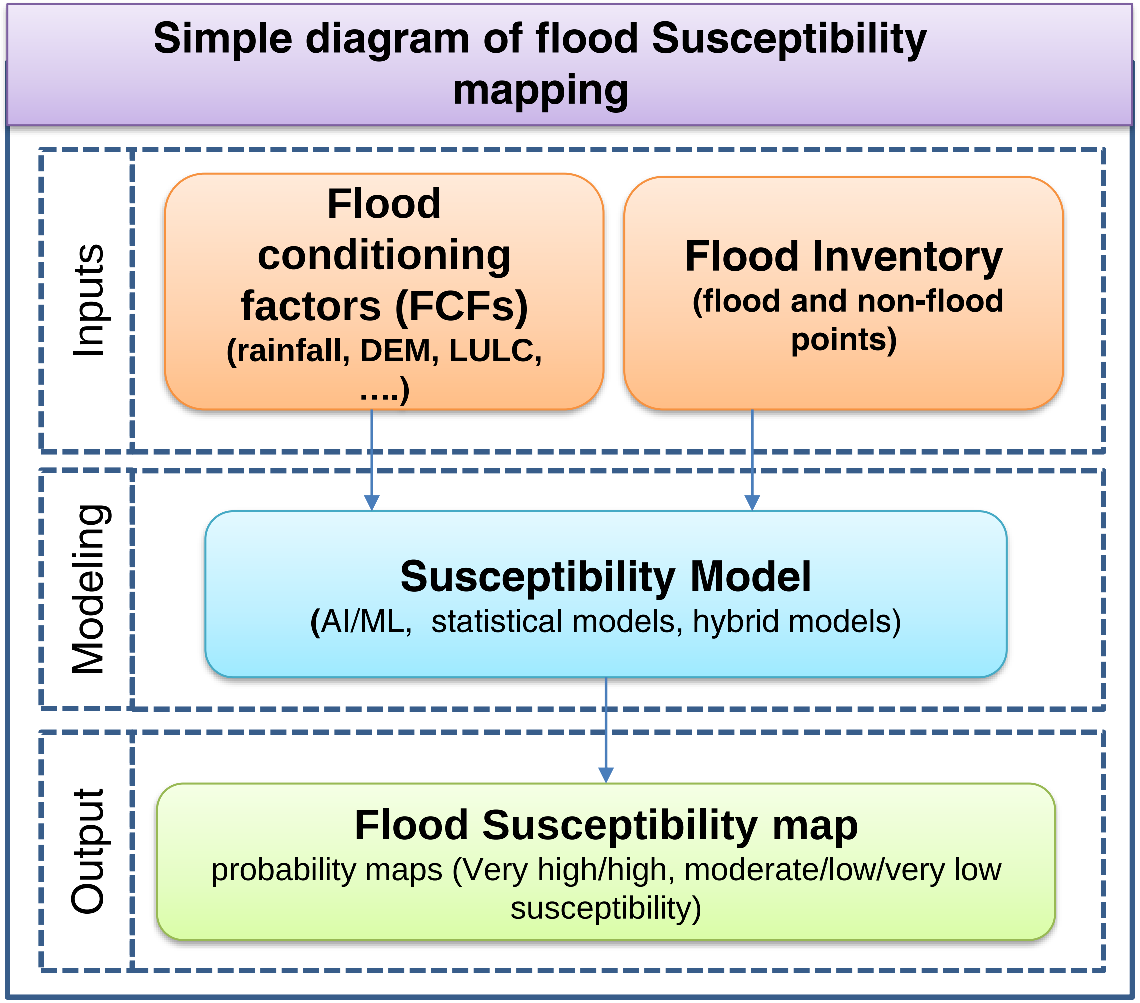

The Role of Flood Inventory in Susceptibility Mapping

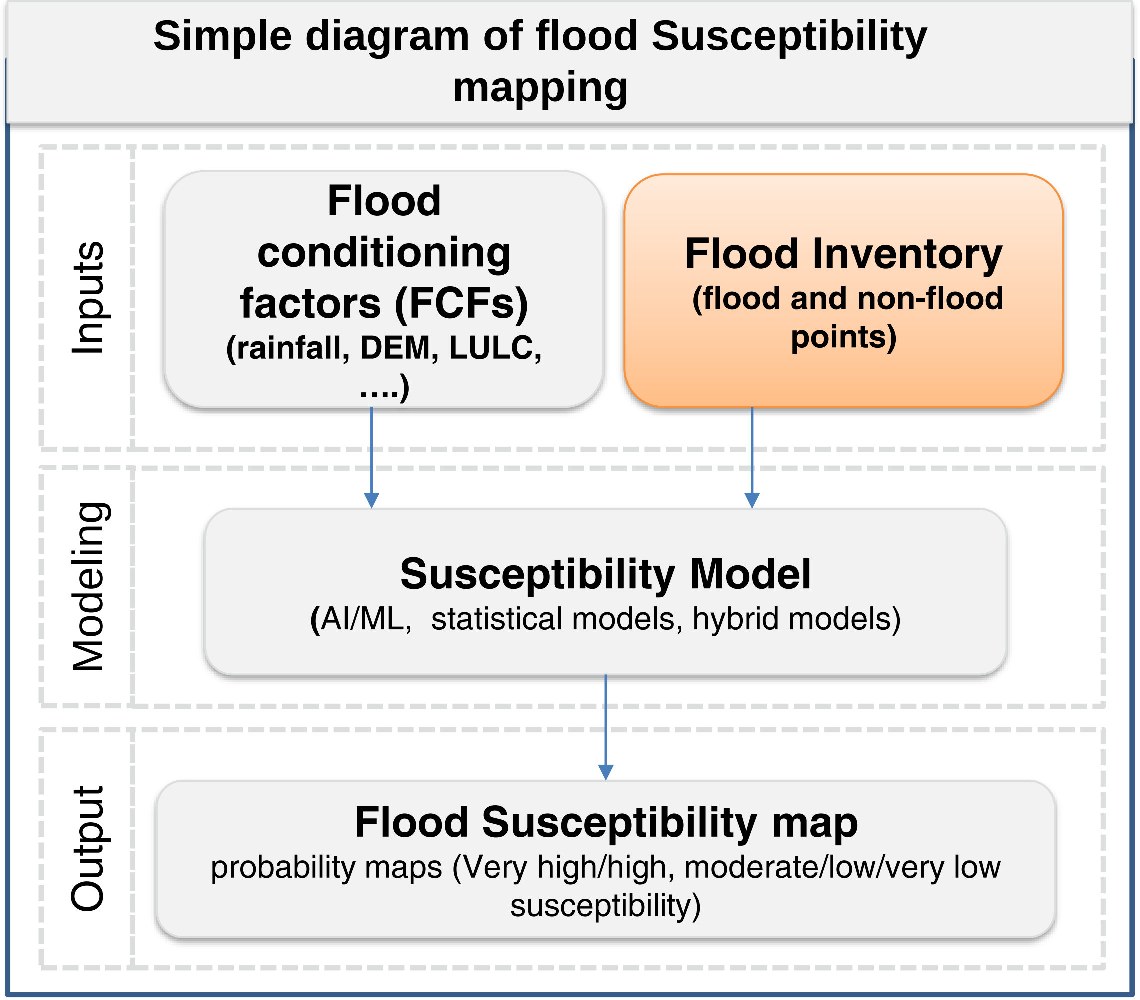

Flood Inventory = Ground Truth

- 📍 Collection of **flood and non-flood points**
- Each point = observed condition (flooded = 1, non-flooded = 0)
- Provides the **training data** for AI/ML and statistical models

Why It's Important:

- 🎯 Defines the "**known reality**" that models learn from
- 🏗 Without accurate inventories, susceptibility maps risk being **unreliable**
- 🔄 Enables **validation** of flood susceptibility predictions
- 🌍 Critical for **scaling models** across regions and climates

Traditional Practice:

- Researchers often relied on:
  - Sparse **ground observations** in affected areas
  - Manual interpretation of satellite images
  - Post-disaster survey data
- Limitations: slow, costly, incomplete

Remote Sensing for Flood Inventory Generation

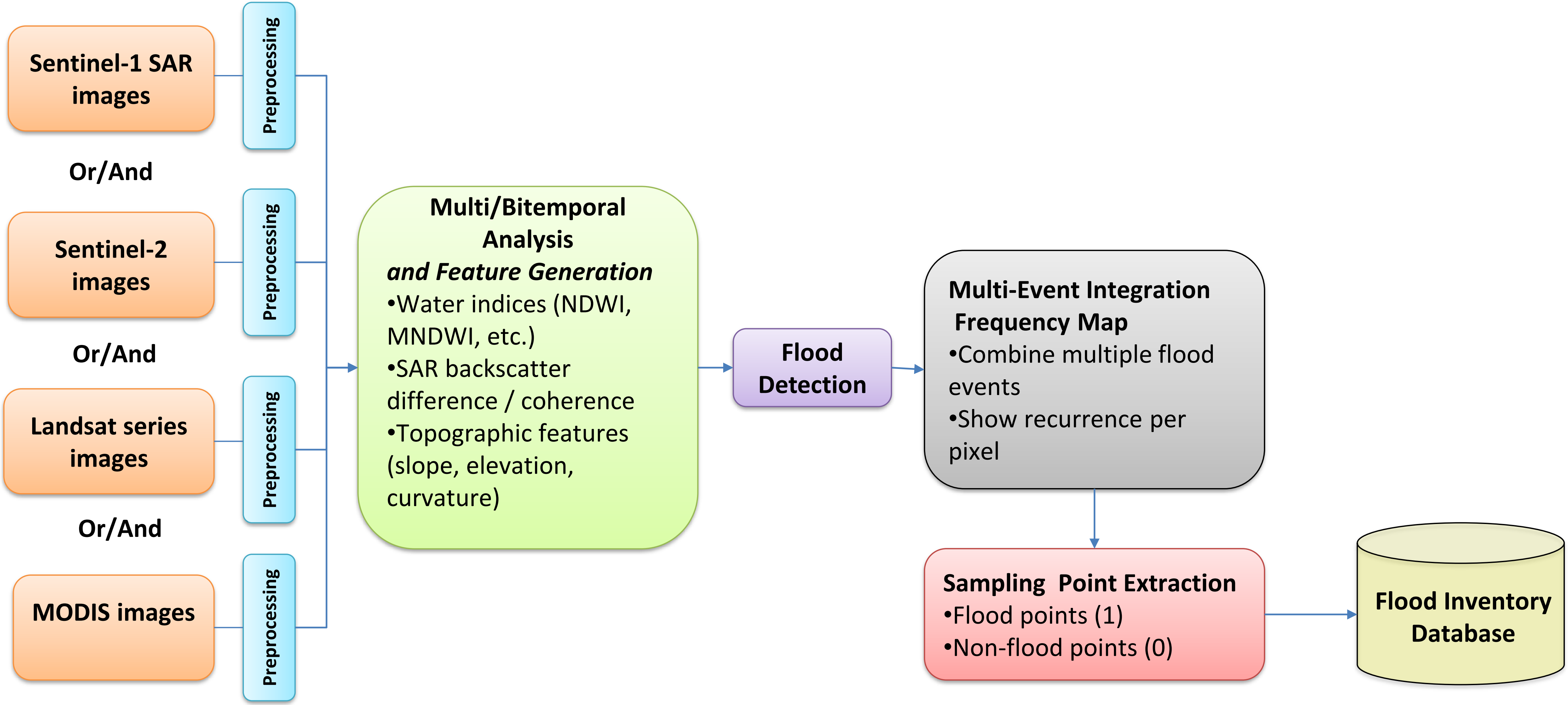

Traditional Core Processing Method for flood inventory generation from remote sensing images: Otsu Thresholding

📊 **Otsu Thresholding**

•**Intensity-based classification** (histogram-driven)
•Finds a **global threshold** that separates pixels into two classes:
- 🌊 Water (flooded)
- 🏔 Non-water (non-flooded)

•Applied to:
- Water indices (NDWI, MNDWI) from optical sensors (Sentinel-2, Landsat)
- SAR backscatter values (Sentinel-1)

• 🌐 Often implemented in **Google Earth Engine (GEE)** for large-scale, rapid mapping
• 💡 Outcome: **binary flood maps** (flood vs non-flood), widely used in operational and academic studies

Otsu-based flood inventory generation using Sentinel-1 SAR data

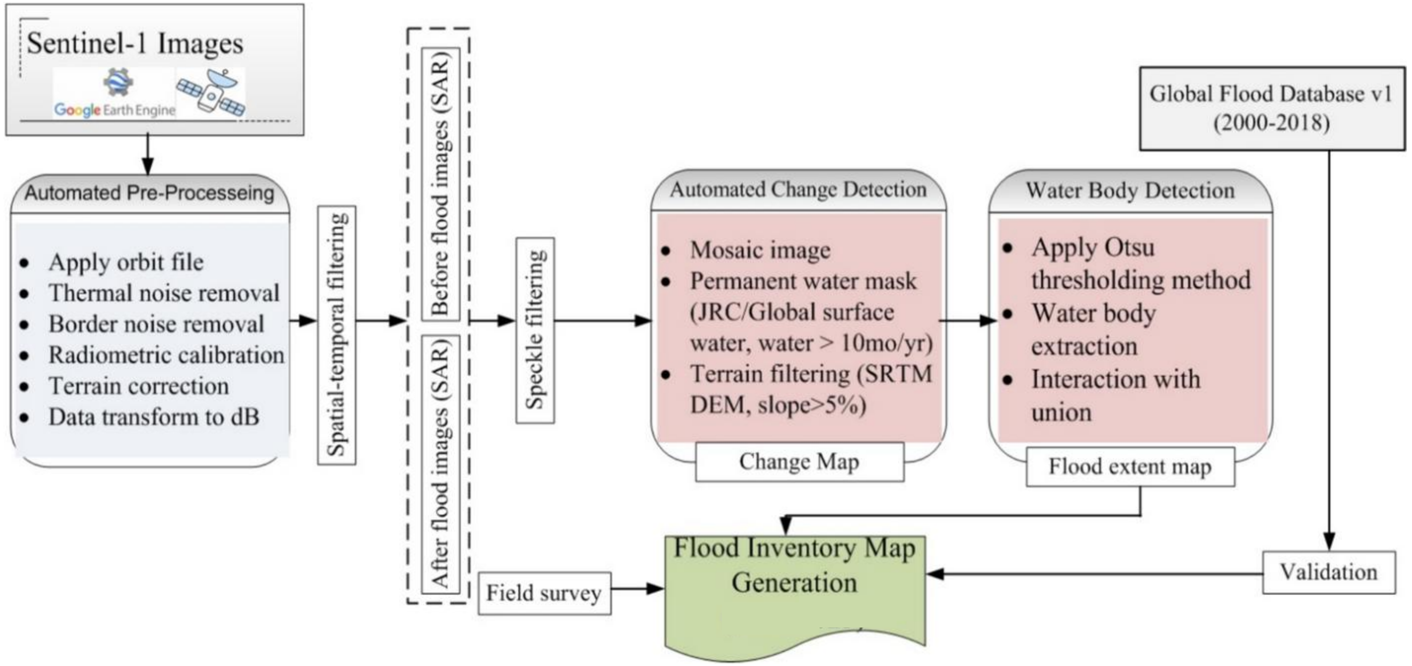

Contents lists available at ScienceDirect

Journal of Hydrology

journal homepage: www.elsevier.com/locate/jhydrol

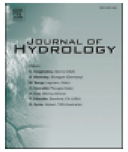

Research papers

Flood susceptibility mapping using multi-temporal SAR imagery and novel integration of nature-inspired algorithms into support vector regression

Soroosh Mehravar[a], Seyed Vahid Razavi-Termeh[b], Armin Moghimi[c,d], Babak Ranjgar[c], Fatemeh Foroughnia[e,*], Meisam Amani[f]

Source: https://doi.org/10.1016/j.jhydrol.2023.129100

Study area: Ahwaz, Khuzestan, Iran

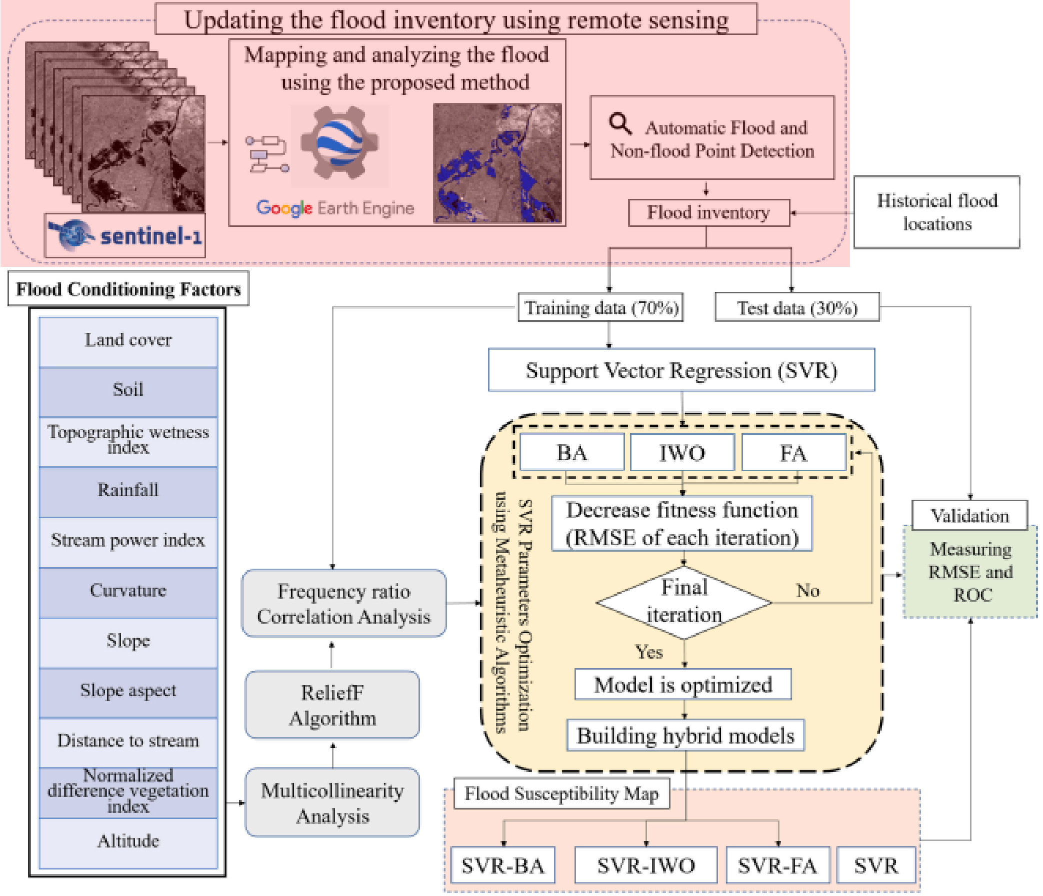

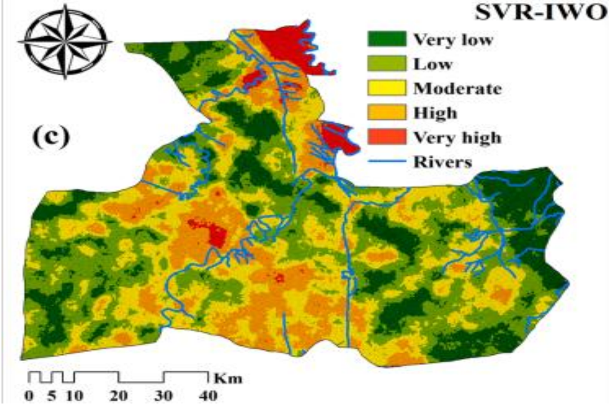

Best model susceptibility Map

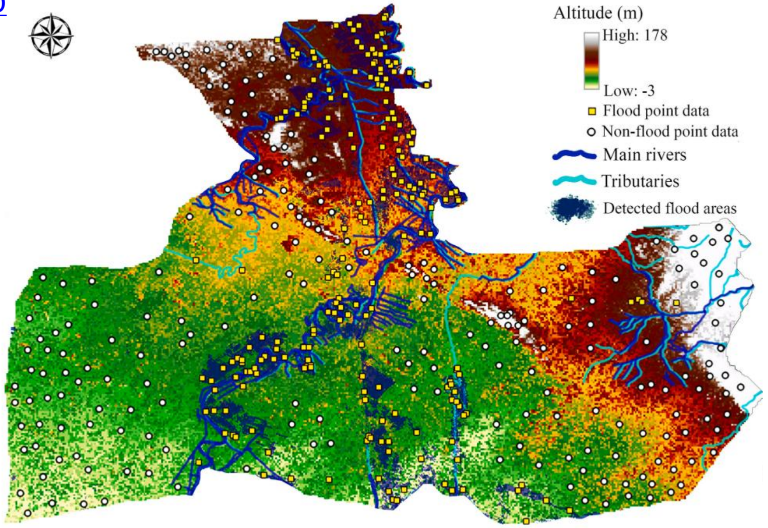

The generated flood inventory map

The results of the area under the ROC curve (AUROC) related to the flood susceptibility models.

Models	AUROC	Standard error	Asymptotic 95 % confidence interval	
			Lower bound	Upper bound
SVR-FA	0.806	0.0319	0.741	0.861
SVRIWO	0.802	0.0323	0.737	0.858
SVR-BA	0.793	0.0334	0.727	0.850
SVR	0.774	0.0346	0.705	0.833

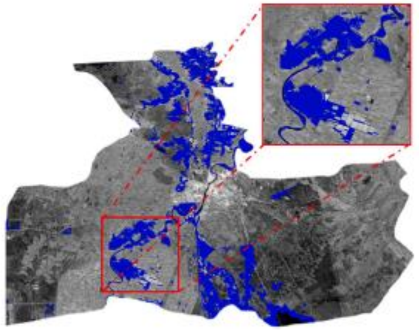

Otsu-based flood map

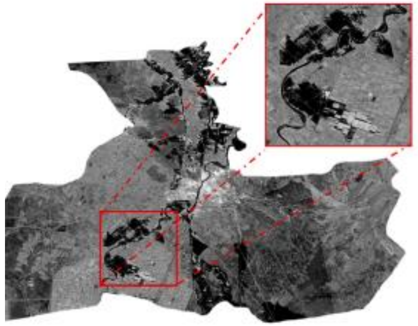

Post-flood SAR image captured by sentinel-1

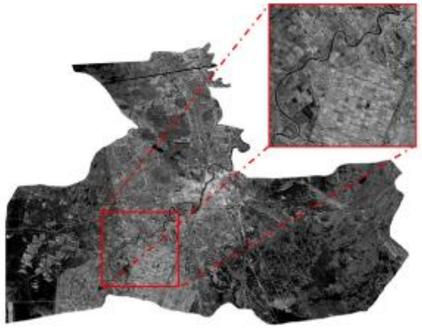

Pre-flood SAR image captured by sentinel-1

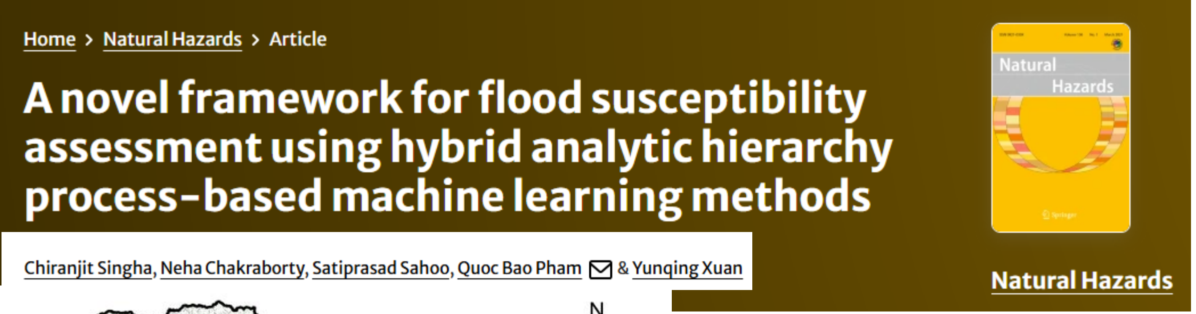

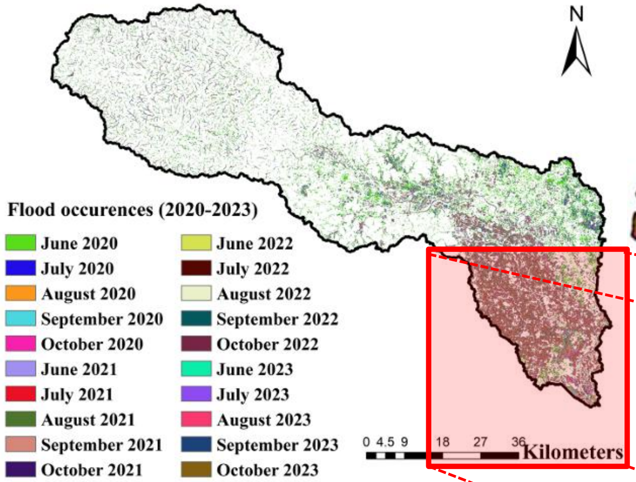

S1C-based historical flood occurrences map generation (2020–2023)

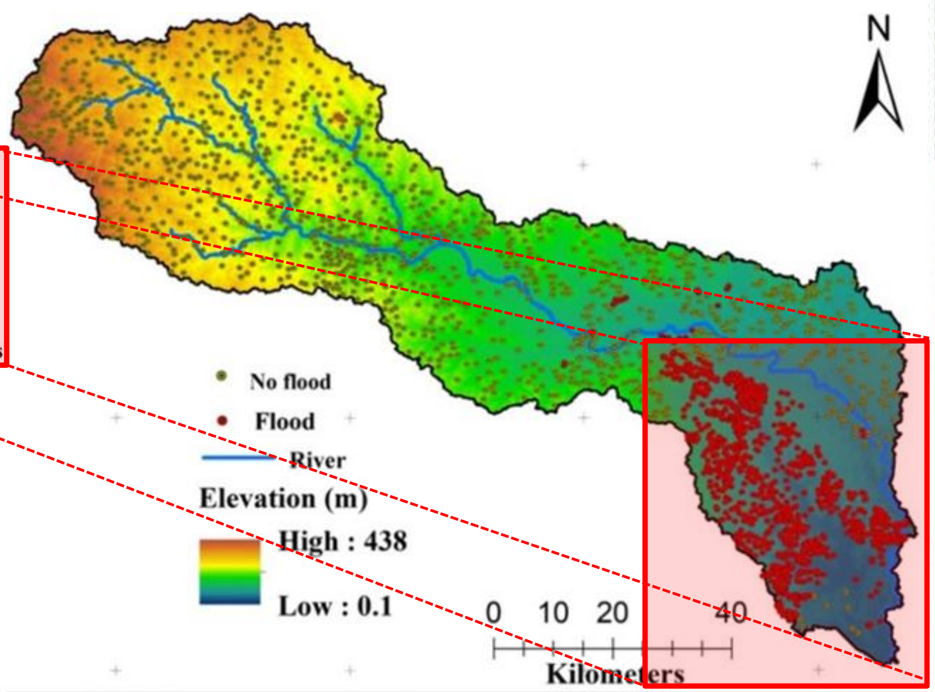

The generated flood inventory map

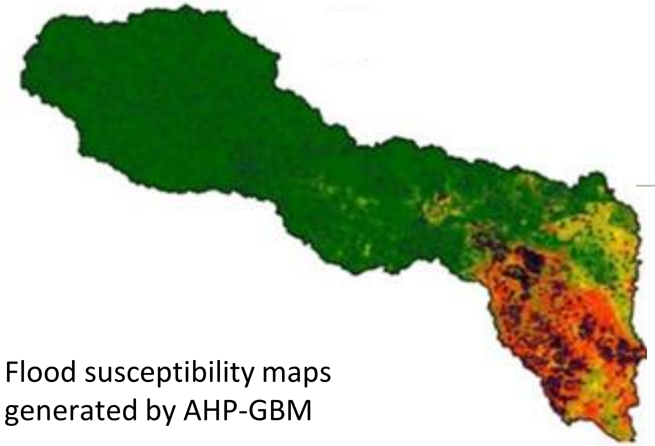

Flood susceptibility maps generated by AHP-GBM

Source: https://doi.org/10.1007/s11069-025-07335-8

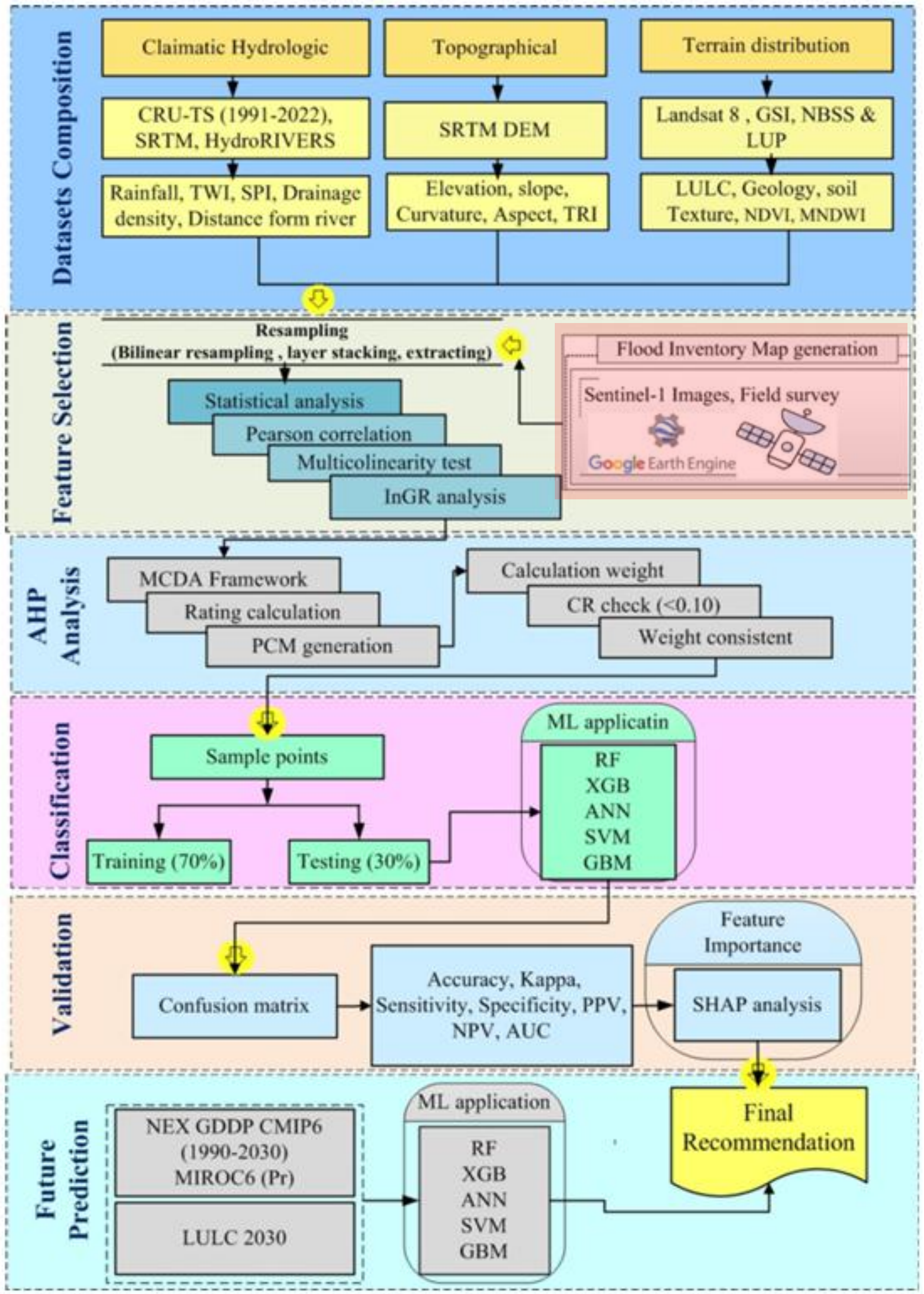

Limitations of Otsu-Based and Traditional ML Models for Flood Inventory

Limitation with Traditional Otsu-Based Approaches

- ⚠ **Global Thresholding Problem** → oversimplifies diverse landscapes
- **Noise Sensitivity** → SAR speckle, vegetation, shadows misclassified

Limitations of Traditional ML Models

- 🕵 **Training Data Dependence**
Results only as good as the inventory used.
- 📊 **Limited Features**
Require manual feature extraction for better performance.
- 🌍 **Low Transferability**
Models often fail outside the training basin.

Toward automated, scalable, and reliable flood inventory generation

AI-driven methods

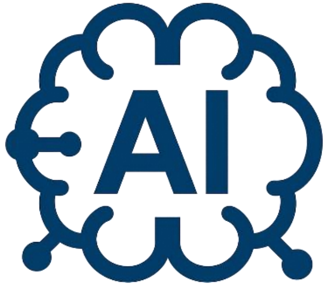

!?

They need a lots of data for effective training

Now, we have a lots of bench Mark Remote sensing dataset for effective training and inferencing.

Some example datasets:

MMFlood **Sen1Floods11**

SEN12-FLOOD **WorldFloods**

AI-Driven Flood Inventory Generation using multisource RS data: Workflow

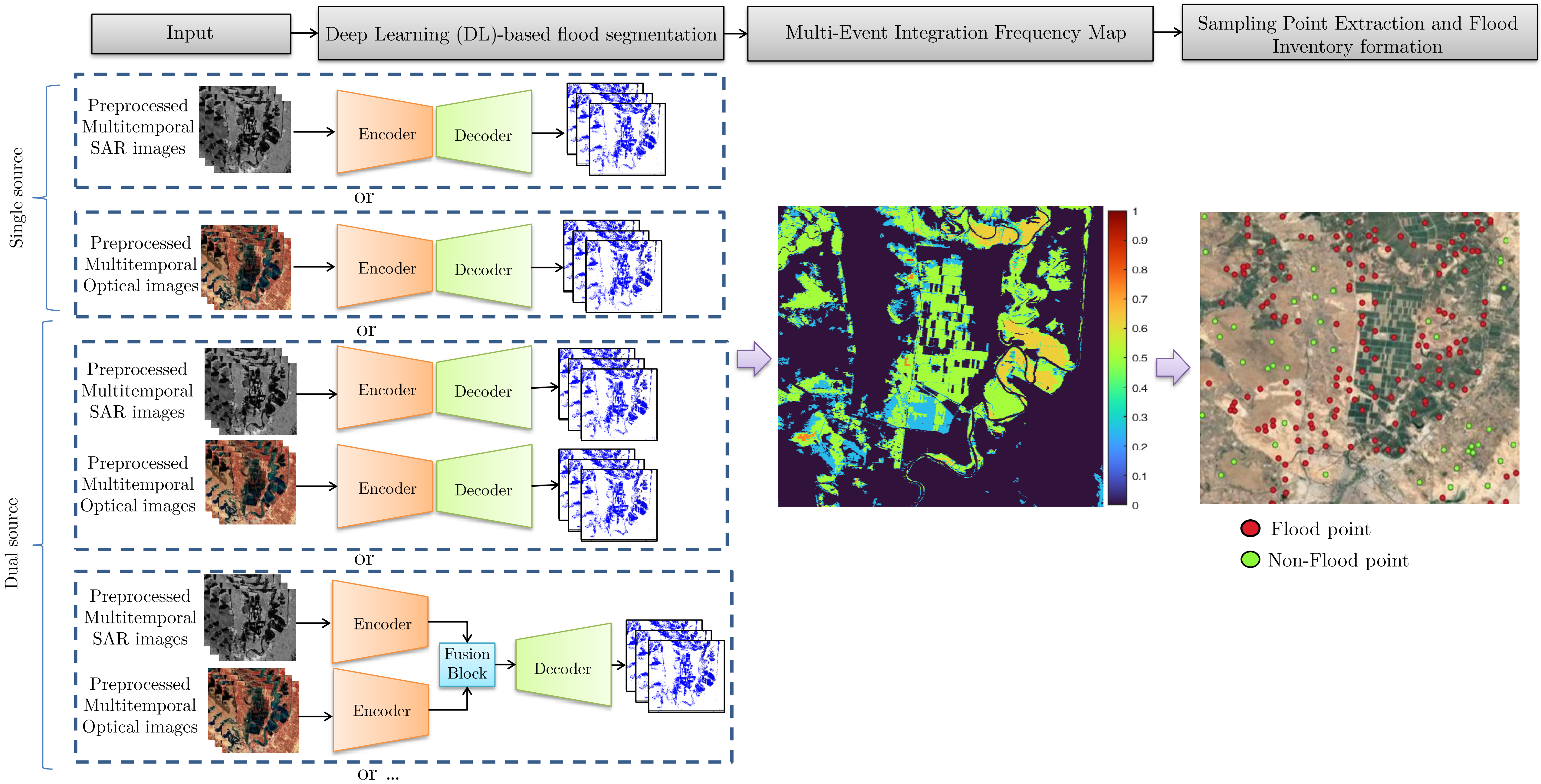

AI-Driven Flood Inventory Generation using multisource RS data: Workflow

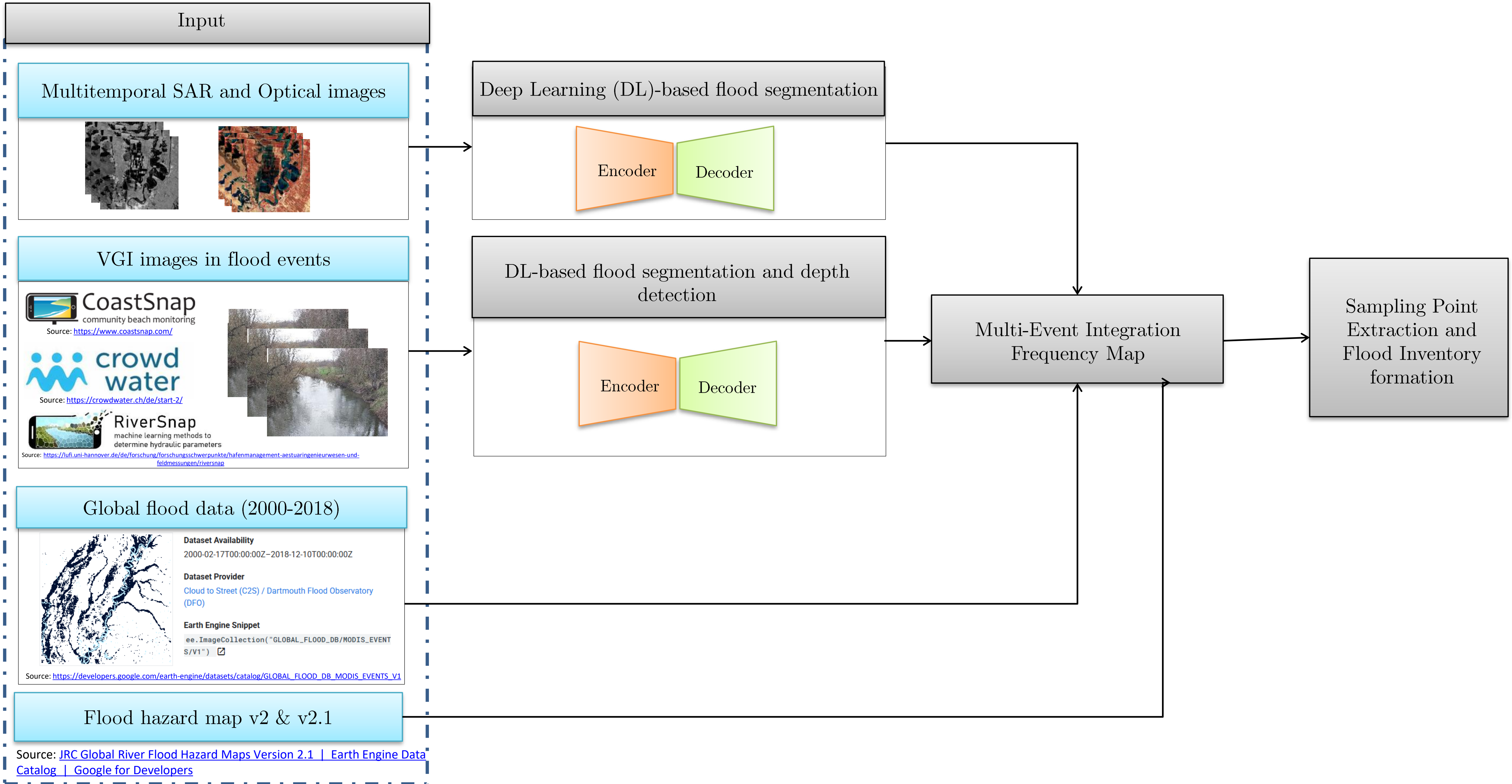

Contents lists available at ScienceDirect

Journal of Environmental Management

journal homepage: www.elsevier.com/locate/jenvman

Research article

Advancing flood risk assessment: Multitemporal SAR-based flood inventory generation using transfer learning and hybrid fuzzy-AHP-machine learning for flood susceptibility mapping in the Mahananda River Basin

Chiranjit Singha [a], Satiprasad Sahoo [b,c], Alireza Bahrami Mahtaj [d], Armin Moghimi [e,*], Mario Welzel [e], Ajit Govind [b]

[a] Department of Agricultural Engineering, Institute of Agriculture, Visva-Bharati (A Central University), Sriniketan, Birbhum, 731236, India
[b] International Center for Agricultural Research in the Dry Areas (ICARDA), 2 Port Said, Victoria Sq, Ismail El-Shaaer Building, Maadi, Cairo, 11728, Egypt
[c] Prajukti Research Private Limited, Baruipur, 743610, West Bengal, India
[d] Faculty of Geodesy and Geomatics Engineering, K. N. Toosi University of Technology, Tehran, 1996715433, Iran
[e] Ludwig-Franzius-Institute for Hydraulic, Estuarine and Coastal Engineering, Leibniz University Hannover, Nienburger Str. 4, 30167, Hannover, Germany

ARTICLE INFO

Handling editor: Jason Michael Evans

Keywords:
Flood susceptibility (FS) mapping
FuzzyAHP
Machine Learning (ML)
Climate change scenarios (SSP2-4.5
SSP5-8.5)
SHAP analysis
Transfer learning
Mahananda River Basin
Flood inventory

ABSTRACT

The Mahananda River basin, located in Eastern India, faces escalating flood risks due to its complex hydrology and geomorphology, threatening socioeconomic and environmental stability. This study presents a novel approach to flood susceptibility (FS) mapping and updates the region's flood inventory. Multitemporal Sentinel-1 (S1) SAR images (2020–2022) were processed using a U-Net transfer learning model to generate a water body frequency map, which was integrated with the Global Flood Dataset (2000–2018) and refined through grid-based classification to create an updated flood inventory. Eleven geospatial layers, including elevation, slope, soil moisture, precipitation, soil type, NDVI, Land Use Land Cover (LULC), geomorphology, wind speed, drainage density, and runoff, were used as flood conditioning factors (FCFs) to develop a hybrid FS mapping approach. This approach integrates the Fuzzy Analytic Hierarchy Process (FuzzyAHP) with six machine learning (ML) algorithms to create hybrid models FuzzyAHP-RF, FuzzyAHP-XGB, FuzzyAHP-GBM, FuzzyAHP-avNNet, FuzzyAHP-AdaBoost, and FuzzyAHP-PLS. Future flood trends (1990–2030) were projected using CMIP6 data under SSP2-4.5 and SSP5-8.5 scenarios with MIROC6 and EC-Earth3 ensembles. The SHAP algorithm identified LULC, NDVI, and soil type as the most influential FCFs, contributing over 60 % to flood susceptibility. Results show that 31.10 % of the basin is highly susceptible to flooding, with the western regions at greatest risk due to low elevation and high drainage density. Future projections indicate that 30.69 % of the area will remain highly vulnerable, with a slight increase under SSP5-8.5. Among the models, FuzzyAHP-XGB achieved the highest accuracy (AUC = 0.970), outperforming FuzzyAHP-GBM (AUC = 0.968) and FuzzyAHP-RF (AUC = 0.965). The experimental results showed that the proposed approach can provide a spatially well-distributed flood inventory derived from freely available remote sensing (RS) datasets and a robust framework for long-term flood risk assessment using hybrid ML techniques. These findings offer critical insights for improving flood risk management and mitigation strategies in the Mahananda River basin.

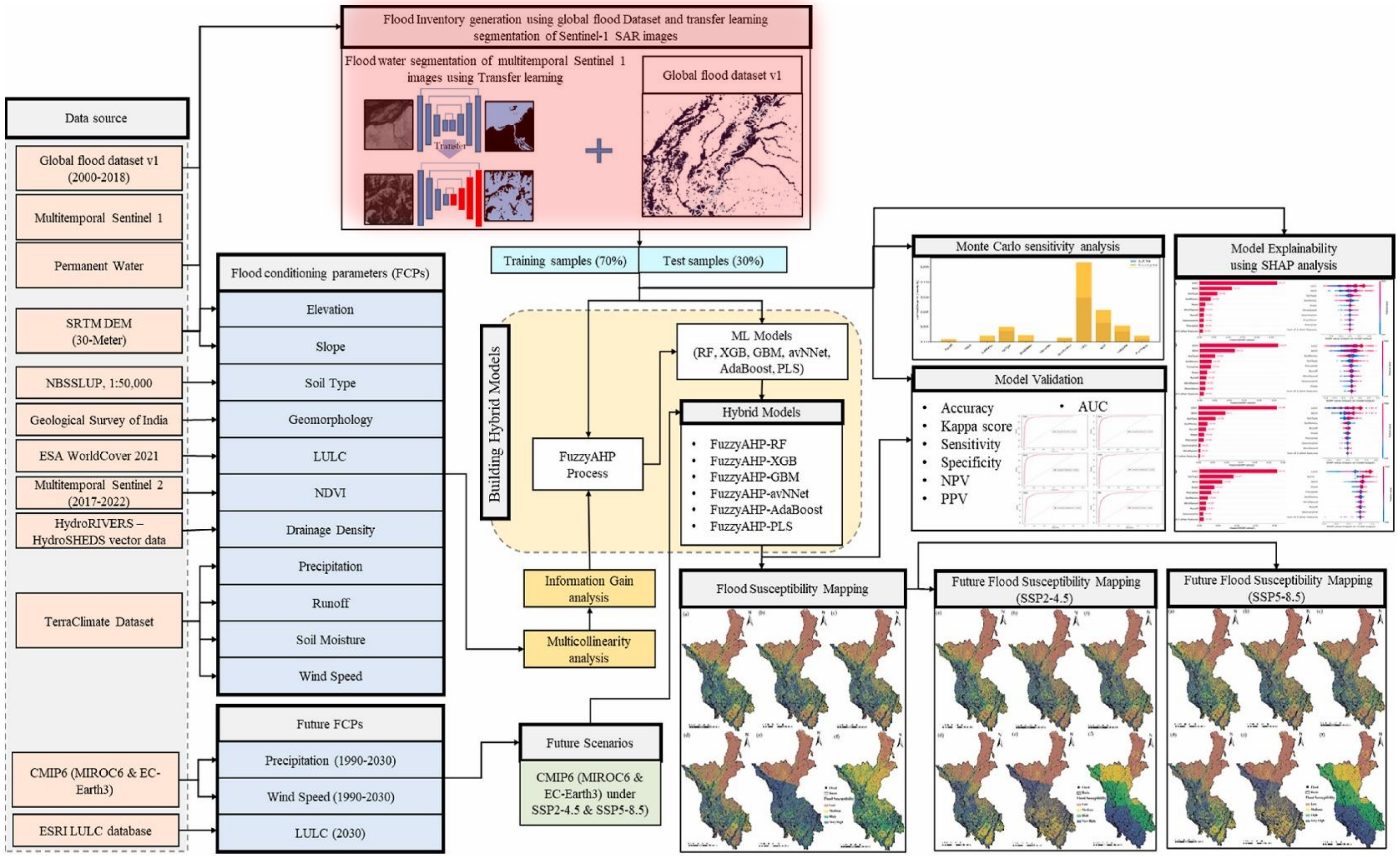

Source: https://doi.org/10.1016/j.jenvman.2025.124972

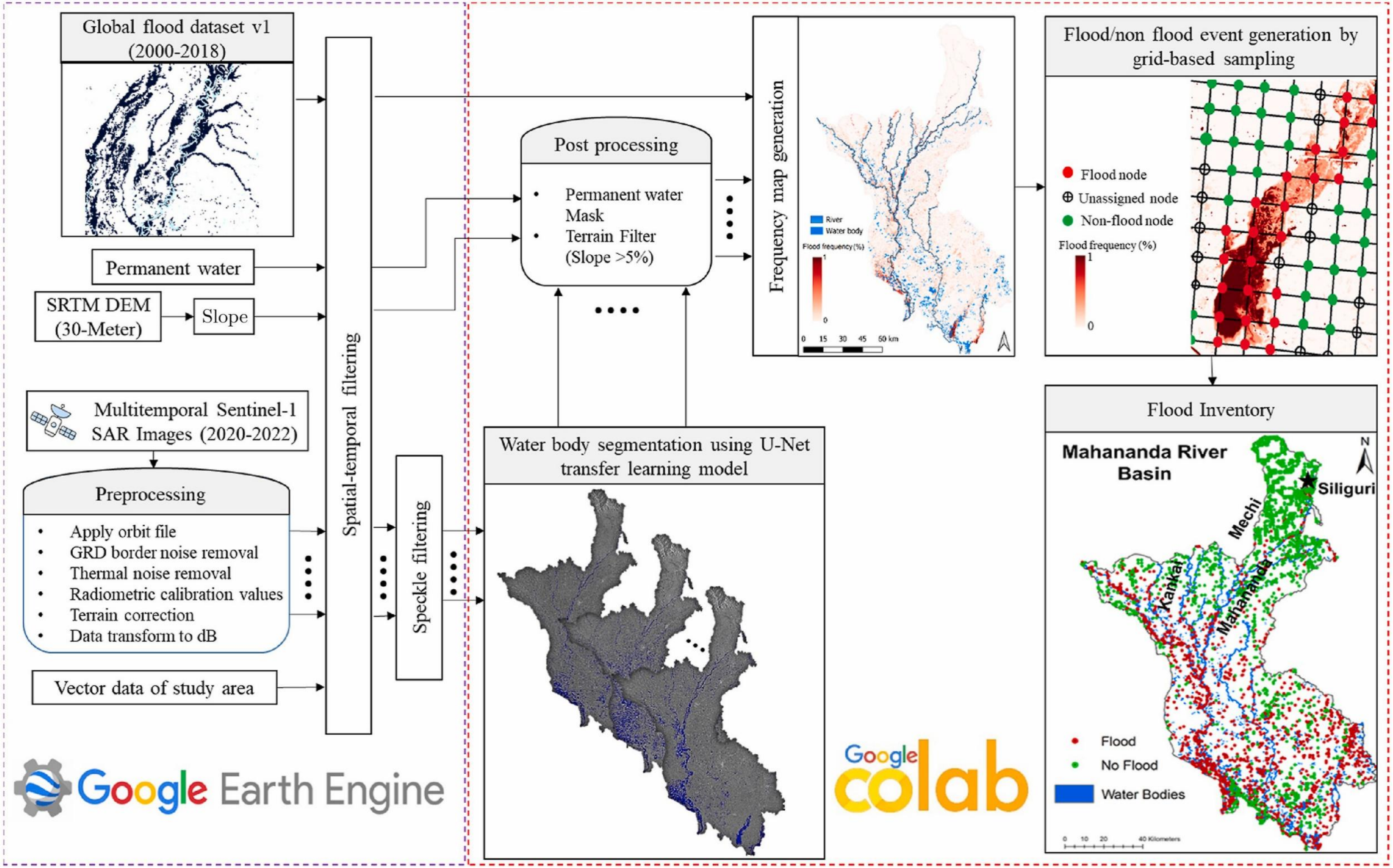
Global flood dataset v1 (2000-2018)
Permanent water
SRTM DEM (30-Meter)
Slope
Multitemporal Sentinel-1 SAR Images (2020-2022)
Preprocessing
Apply orbit file
GRD border noise removal
Thermal noise removal
Radiometric calibration values
Terrain correction
Data transform to dB
Vector data of study area
Spatial-temporal filtering
Speckle filtering
Post processing
Permanent water Mask
Terrain Filter (Slope >5%)
Water body segmentation using U-Net transfer learning model
Frequency map generation
River
Water body
Flood frequency (%)
Flood/non flood event generation by grid-based sampling
Flood node
Unassigned node
Non-flood node
Flood frequency (%)
Flood Inventory
Mahananda River Basin
Siliguri
Mechi
Kankai
Mahananda
Flood
No Flood
Water Bodies
Google Earth Engine
Google colab

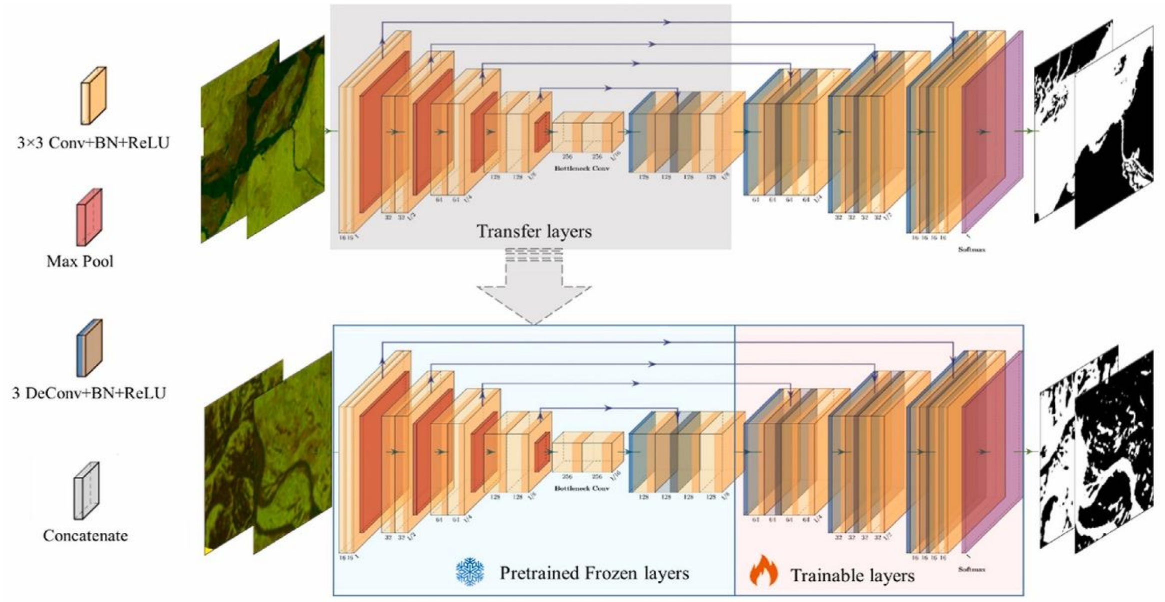

Number of Parameters and Training Time per Epoch for considered model.

Model	Total Parameters	Trainable Parameters	Non-trainable Parameters	Time per Epoch (*s*)
U-Net	1,945,969	1,943,537	2432	3.56
Transfer U-Net	1,945,969	1,353,377	592,592	1.26
V-Net	18,436,017	18,430,385	5632	6
Attention U-Net	10,161,060	10,153,636	7424	5.9
U-Net++	8,569,537	8,562,113	7424	4.7
U-Net 3+	1,972,513	1,968,865	3648	3.6

Performance comparison of considered segmentation models in water body detection form S1 SAR images (red: best performance, blue: second best performance).

Model	IoU	Recall	Accuracy	Precision	F1-score
U-Net	0.898	0.932	0.979	0.961	0.946
V-Net	0.888	0.902	0.978	0.983	0.941
Attention U-Net	0.906	0.929	0.981	0.973	0.951
U-Net++	0.877	0.936	0.974	0.932	0.934
U-Net 3+	0.902	0.962	0.980	0.935	0.949
Transfer U-Net	0.914	0.960	0.982	0.949	0.954

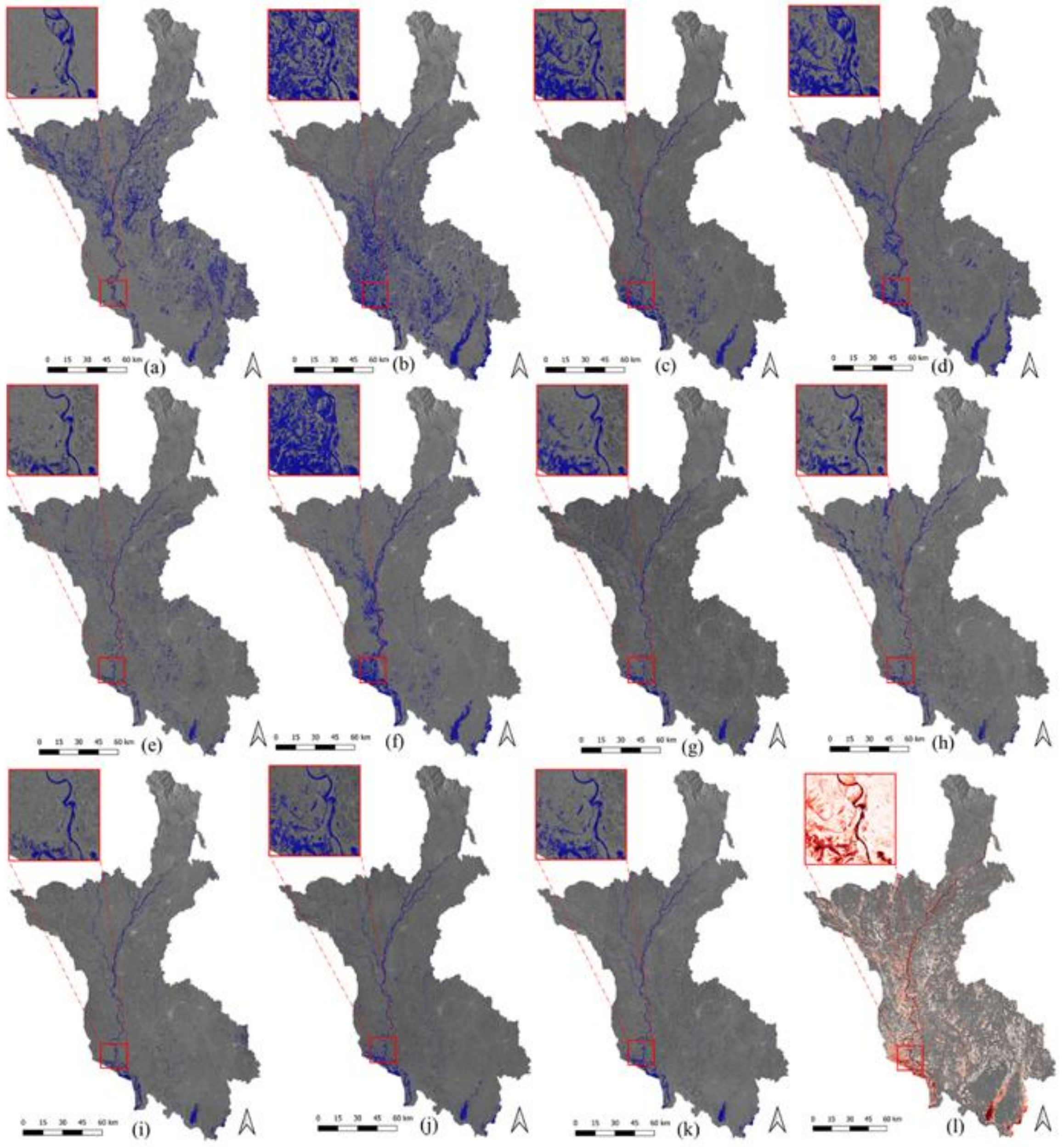

Fig. 7. Water bodies detected by Transfer U-Net from S1 images acquired post-flood on (a) 2020/06/27, (b) 2020/07/27, (c) 2020/08/31, (d) 2020/09/24, (e) 2021/07/28, (f) 2021/08/26, (g) 2021/09/26, (h) 2021/10/25, (i) 2022/08/28, (j) 2022/09/26, (k) 2022/10/27, and (l) frequency water body map generated by stacking all detected water bodies from SAR images with the Global Flood Dataset v1 (2000–2018), superimposed on a SAR image. The blue is water body.

Source: https://doi.org/10.1016/j.jenvman.2025.124972

Flood/Non-Flood Point Derivation in the paper

Step 1: Flood Frequency from Sentinel-1 SAR

$$F_{\text{freq}} = \frac{1}{N_s} \sum_{j=1}^{N_s} F_j$$

- N_s: number of Sentinel-1 images
- F_j: flood map from the j^{th} SAR acquisition
- Output: **flood frequency map** (probability of flooding per pixel)

Step 2: Integration with Historical Database (GFD v1)

$$F_{\text{freq}}^{U} = \frac{F_{\text{freq}} + F_{\text{GFD}}}{2}$$

- Combine Sentinel-1 frequency map with **Global Flood Database (2000–2018)**
- Output: **updated flood frequency map** F_{freq}^{U}

Step 3: Grid-Based Sampling with k-NN

At each grid node $g \in G$:

$$\bar{F}(g) = \frac{1}{k} \sum_{i=1}^{k} F_{\text{freq}}^{U}(g_i)$$

- Use **k nearest neighbors (k = 25)** via KD-tree
- Compute **average flood frequency** of neighbors

Step 4: Classification Rule

$$F_{\text{refined}}(g) = \begin{cases} \textbf{Flood}, & \bar{F}(g) \geq 0.80 \\ \textbf{Non-Flood}, & \bar{F}(g) < 0.10 \\ \textbf{Unassigned}, & 0.10 \leq \bar{F}(g) < 0.80 \end{cases}$$

- Output: **refined flood inventory** (flood & non-flood points)

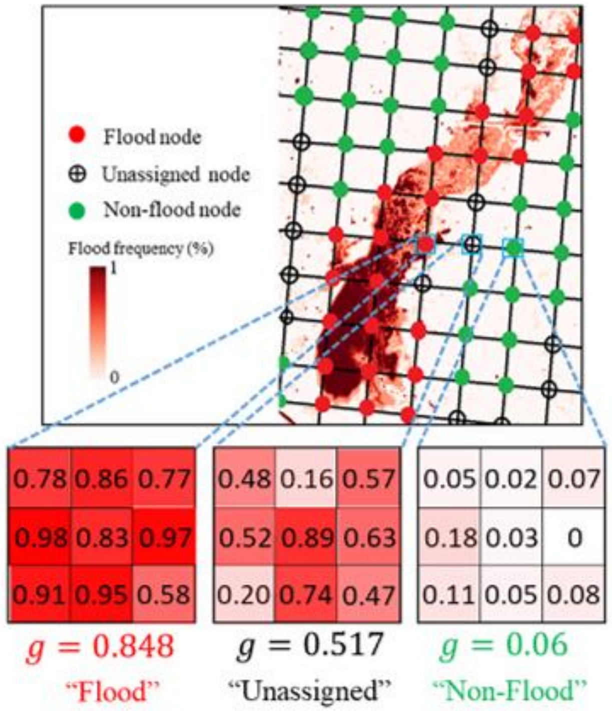

Example of proposed grid-based sampling approach for generating flood and non-flood points when k=9. Source: https://doi.org/10.1016/j.jenvman.2025.124972

Overall process and Results

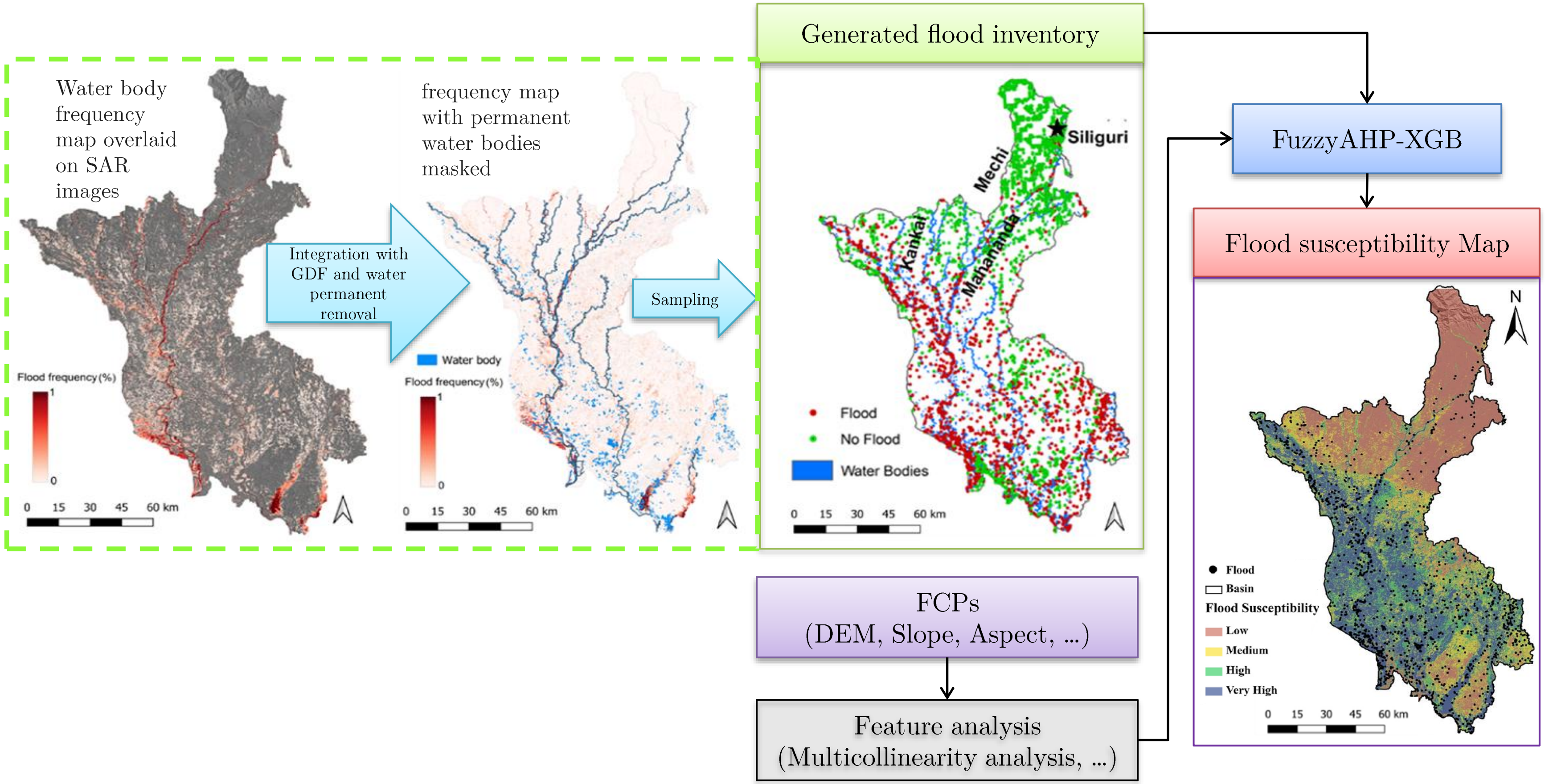

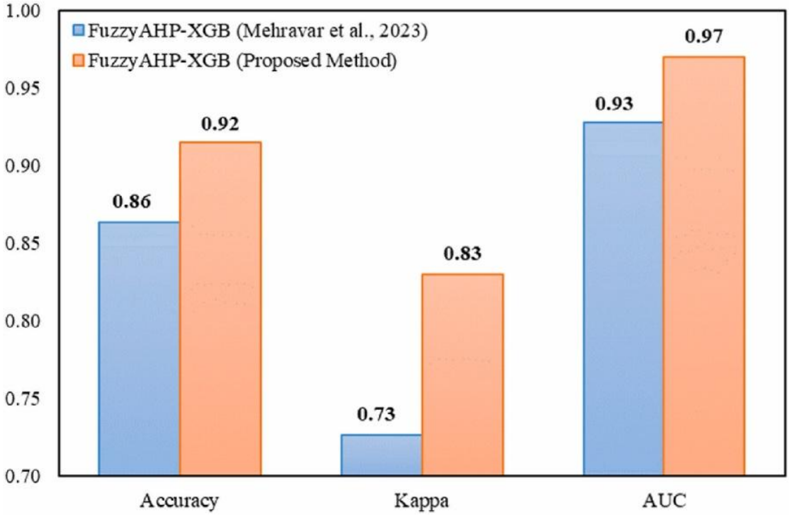

Comparative performance analysis of the FuzzyAHP-XGB (proposed method) and the FuzzyAHP-XGB (Mehravar et al., 2023) approach.

Source: https://doi.org/10.1016/j.jenvman.2025.124972

Conclusion and Future Work

Conclusion

•Flood susceptibility mapping **depends heavily on flood inventory quality**.

•Traditional methods (Otsu, classical ML) are **limited** by noise sensitivity, weak transferability, and oversimplified thresholds.

•**AI-driven approaches** using deep learning and multi-source data provide **more reliable and scalable inventories**, significantly improving susceptibility model performance.

Future Work

- 🌐 **Multi-Source Fusion**: Integrate SAR, optical, DEM, hydrologic, and citizen science data.
- 🔍 **Advanced Sampling**: Explore adaptive or uncertainty-driven methods for inventory refinement.
- 🤝 **Collaborative Science**: Combine global datasets with local knowledge for more inclusive flood risk mapping.

Thank you !

If you have questions or would like to collaborate, feel free to contact me:

:Moghimi.armin@gmail.com